A Tool for Small-Signal Stability Analysis of Low Voltage DC Network

Qihao Guo, Jérôme Buire, David Frey, Patrick Chambon

A Tool for Small-Signal Stability Analysis of Low Voltage DC Network

Qihao Guo[1], Jérôme Buire[1], David Frey[1], and Patrick Chambon[2]

[1]Univ. Grenoble Alpes, CNRS, Grenoble INP**, G2ELab, 38000 Grenoble, France
**Institute of Engineering Univ. Grenoble Alpes
[2] Schneider Electric, Electropole, 38320 Eybens, France

Abstract – This paper presents a tool for small-signal stability analysis of low-voltage DC network. This tool includes both modal analysis and impedance-based method, providing complementary insights into the small-signal stability problem in both time and frequency domains, like stability margin, oscillation modes, and participation factors. This tool covers different commonly used DC-DC converters with closed-loop controllers, such as the boost and the buck DC-DC. Some typical case studies are presented to illustrate the capability and suitability for research purposes.

Key words – low voltage DC microgrid,DC-DC converter, small-signal stability, modal analysis, impedance method

1. INTRODUCTION

Recently, the small-signal stability issue has become increasingly common in low-voltage direct current (LVDC) microgrids (MGs) and is drawing growing attention from researchers, equipment manufacturers, and system operators. This instability is characterized by the growing oscillations of state variables, like the DC bus voltage, when the system is subjected to "small" perturbations, such as a slight load variation. These undesired oscillations can significantly degrade the power quality and result in overvoltage, which is harmful to devices connected to the DC bus.

A small-signal stability analysis is necessary for evaluating and understanding the root causes of oscillation risks. Indeed, in a complex LVDC MG, there are multiple state variables, and each of them may have a different contribution to the instability. Understanding the relative participation of these state variables to specific oscillatory modes is essential for operators to figure out solutions to enhance the system stability.

However, conducting a thorough small-signal stability analysis is not a trivial task due to the limited available tools, especially for LVDC MGs. The traditional solution is to use the commercial software, e.g., Simulink. It follows an "all-in-one" philosophy and is generally well-tested and user-friendly. Besides, it is powerful enough to conduct time-domain simulation ; therefore, the user can easily visualize oscillation waveforms when instability occurs. However, this kind of software is "closed", i.e., users do not have the right to get access to the state variables. Consequently, adding user-defined algorithms, such as modal analysis, is difficult.

Recently, open-source research tools developed in high-level scientific languages such as MATLAB and Python have become increasingly preferred. Among them, MatPower [1] and pandapower [2] are two typical open-source and freely downloadable tools. However, both of them are designed for AC steady-state analysis, like the power flow study, without a small-signal stability analysis toolbox. To handle this problem, researchers have developed specific tools for stability analysis, such as G2ELin [3], SimplusGT [4], and PSAT [5]. They are open-source MATLAB-based tools that facilitate dynamic analysis and time-domain simulation of power system with a high penetration of inverter-based resources. For instance, G2ELin includes modal analysis toolboxes, and SimplusGT supports impedance-based root-cause analysis. These tools are primarily designed for AC power systems and do not provide detailed modeling of DC networks, particularly DC-DC converters and cables. For high-voltage direct current (HVDC) transmission systems, open-source tools such as the Z-tool [6] have been developed. The Z-tool is a Python-based implementation for frequency-domain analysis of electrical energy hubs, with core functionalities including admittance characterization and small-signal stability assessment. Table 1 presents a comparison of various tools based on their functionalities for small-signal stability analysis. The comparison criteria include the programming language used, the type of stability analysis tools offered, and their applicability to AC or DC power systems.

However, to the best of the authors' knowledge, no comparable tools have been developed specifically for LVDC applications. In fact, LVDC networks are promising candidates for future power supply systems for applications such as data centers, which accounted for roughly 1.5% of global electricity consumption in 2024 and these facilities will use twice as much energy by 2030 - driven by artificial intelligence [8]. Furthermore, DC microgrids can also be applied in rural areas, such as in countries in Africa where access to reliable and affordable electricity is challenging [9, 10].

For the above consideration, this paper presents a Matlab-based tool aiming at providing a small-signal stability analysis solution especially for LVDC MG. This tool has three main features :

- Special attention is given to the modelling of DC elements commonly used in LVDC applications, such as the DC-DC converter under different control modes, DC cables and DC loads.
- Modal analysis algorithm is integrated, which provides toolboxes like eigenvalues, mode shapes, participation factors and parameter sensitivity.
- Impedance-based method for frequency-domain stability analysis of multi-converter systems.

2. MODELS AND ALGORITHMS

2.1. *Network topology definition*

Three types of data matrices are used to store the information of the network topology. The choice of these data matrices is analogous to the design philosophy of some open-source software, like Matpower [1].

The three data matrices are :

- bus matrix : contains the DC bus data. The first column indicates the bus number and the second gives the bus type.

TABLEAU 1. A comparison of different open-source software for power system stability analysis
(The symbol ✓ indicates that the function is supported, while ✗ denotes that it is not supported.)

Name	Language	Power flow	Time-domain simulation	Modal analysis	Impedance method	Power system
MatPower [1]	Matlab	✓	✗	✗	✗	AC/DC
PandaPower [2]	Python	✓	✗	✗	✗	AC/DC
G2ELin [3]	Matlab	✓	✓	✓	✗	AC
SimplusGT [4]	Matlab	✓	✓	✓	✓	AC
PSAT [5]	Matlab	✓	✓	✓	✗	AC/DC
Z-tool [6]	Python	✓	✓	✗	✓	HVDC
ANEDS [7]	Python	✓	✓	✓	✗	AC/DC
This paper	Matlab	✓	✓	✓	✓	LVDC

Until now, there are in total 6 bus types [1].

TABLEAU 2. Bus Data Format (`MPC.bus`)

Column	Description	Unit
1	Bus number	integer
2	Bus type	integer

— branch matrix : describes how DC buses are interconnected with each other by lines. Line parameters, such as resistance, inductance, distance are taken into account.

TABLEAU 3. Branch Data Format (`MPC.branch`)

Column	Description	Unit
1	From bus	integer
2	To bus	integer
3	Line resistance	Ω
4	Line inductance	H
5	Line distance	m

— generation matrix : contains all the generation/consumption information of each bus. For the generation bus, information such as the bus reference voltage and droop coefficient is provided. For the consumption bus, information such as load power, load resistance, or load current is provided, depending on the load type.

2.2. *Individual element*

An individual element refers to an electrical apparatus that either connects to a single DC bus (e.g., a DC-DC source/load converter) or interconnects multiple DC buses (e.g., a cable). An individual element is represented by the general block shown in Fig.1.

1. type 1 constant power source, type 2 V-I droop controlled source, type 3 V-P droop controlled source, type 4 constant power load, type 5 constant current load, type 6 constant resistance load.

TABLEAU 4. Generation Data Format (`MPC.gen`)

Column	Description	Unit
1	Bus number	integer
2	Generation/consumption power	W
3	Bus type	integer
4	Droop coefficient	Ω
5	Reference voltage	V
6	Load resistance	Ω
6	Load current	A

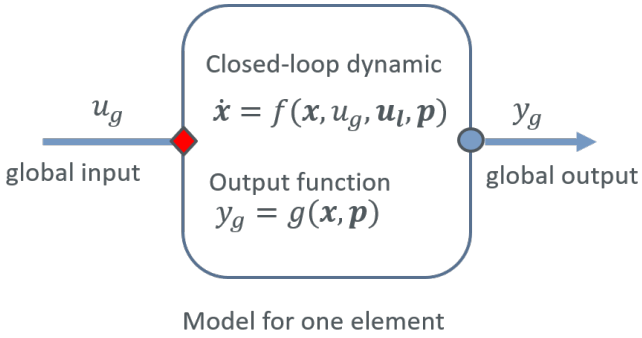

FIG. 1. The representation of the individual element

In fact, each individual element has one global input u_g and one global output y_g, both of which are electrical variables, either voltage or current. If the global input is voltage, then, the global output is automatically current, and vice versa. This design consideration ensures physical causality.

The local input vector $\boldsymbol{u_l}$ refers to the control reference of the closed-loop controlled equipment, for example, the reference voltage, current or power of the DC-DC converter. Passive components, such as DC cables, do not have a local input.

The vector $\boldsymbol{p}$ represents the physical parameters of the element, such as inductance, capacitance, resistance. For the closed-loop controlled system, $\boldsymbol{p}$ also contains the controller parameters.

The dynamic behaviour of the individual element is described by the differential equations $\boldsymbol{f}$. For instance, the cable's dynamic is represented by a first-order RL equivalent. As for closed-loop controlled equipment, such as DC-DC converters, these differential equations contain both the controller and the passive components (inductance/capacitance) dynamic behaviour.

An algebraic equation g describes the relationship between the global output y_g and the state variables $\boldsymbol{x}$ and parameters $\boldsymbol{p}$.

For example, the cable is represented by this modeling method, as shown in Fig.2.

2.3. *Construct the whole system by interconnecting the individual element*

In a complex LVDC MG, there are generally several kinds of individual elements, e.g., multiple source converters supply electrical power to loads by the cables.

In fact, all these individual elements are associated with each other, i.e., the global input of one element is the combination of the global outputs of other elements, based on the network topology information. This can be calculated from bus data (`MPC.bus`) and the branch data (`MPC.branch`). This process is automatically completed by the self-developped function `makeCbus`. A whole system model is then constructed, with state variables, local inputs, and parameters formed by combining those of the individual elements. Indeed, the global in-

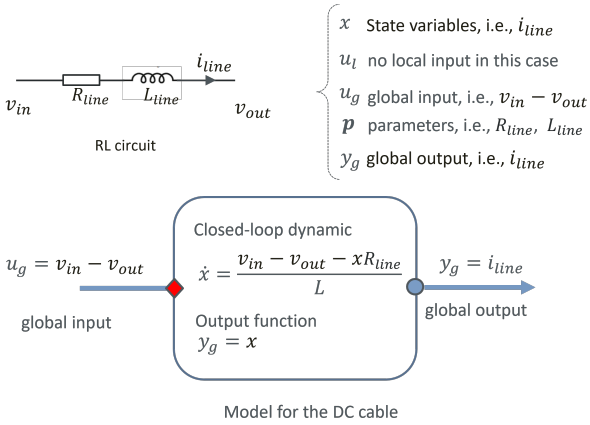

FIG. 2. The representation of the DC cable

put/output of each individual element no longer exists in the whole system, as it operates as a closed-loop. Consequently, the entire MG is represented by the following nonlinear differential equations :

$$\dot{\boldsymbol{x}}_{\text{tot}} = f(\boldsymbol{x}_{\text{tot}}, \boldsymbol{u}_{\text{tot}}, \boldsymbol{p}_{\text{tot}}) \tag{1}$$

$$\boldsymbol{y}_{\text{tot}} = g(\boldsymbol{x}_{\text{tot}}, \boldsymbol{u}_{\text{tot}}, \boldsymbol{p}_{\text{tot}}) \tag{2}$$

where $\boldsymbol{x}_{\text{tot}}$, $\boldsymbol{u}_{l_{\text{tot}}}$, $\boldsymbol{p}_{\text{tot}}$ are the state variables, local inputs, parameters of the whole system.

2.4. *Time-domain simulation*

Equation 1 represents the dynamic behavior of the entire network, which can be solved using various numerical integration methods. In this work, the classical Runge–Kutta method is employed. The objective of conducting time-domain simulation is twofold : 1) help users visualize and analyze the oscillation waveforms if the system is poorly damped and a specific mode is excited. 2) obtain the steady-state values $\boldsymbol{x}_{\text{tot}_0}$. In fact, $\boldsymbol{x}_{\text{tot}_0}$ can be obtained by simulating the system over a sufficient time span and observing when the response reaches equilibrium point.

2.5. *System linearization around the operating point.*

Around the given operating point, the dynamic of the nonlinear whole system can be represented in a linear state-space formulation as follows

$$\Delta\dot{\boldsymbol{x}}_{tot} = \boldsymbol{A}_{tot}\Delta\boldsymbol{x}_{tot} + \boldsymbol{B}_{tot}\Delta\boldsymbol{u}_{tot} \tag{3}$$

$$\Delta\boldsymbol{y}_{tot} = \boldsymbol{C}_{tot}\Delta\boldsymbol{x}_{tot} + \boldsymbol{D}_{tot}\Delta\boldsymbol{u}_{tot} \tag{4}$$

where $\boldsymbol{A}_{tot}$ is the control matrix of size $n_x \times n_x$, $\boldsymbol{B}_{tot}$ is the input matrix of size $n_x \times n_u$, $\boldsymbol{C}_{tot}$ is the output matrix of size $n_y \times n_x$ and $\boldsymbol{D}_{tot}$ is the feedforward matrix of size $n_y \times n_u$. Their analytical expressions can be obtained by linearizing eq.1 around the operating point. This process can be simply achieved by the Matlab function `jacobian`. For instance, $\boldsymbol{A}_{tot}$ is obtained by computing the Jacobian matrix of symbolic function $\boldsymbol{f}$ with respect to state variable $\boldsymbol{x}_{\text{tot}}$, given as

$$\boldsymbol{A}_{tot} = \frac{\partial \boldsymbol{f}}{\partial \boldsymbol{x}_{\text{tot}}}, \boldsymbol{B}_{tot} = \frac{\partial \boldsymbol{f}}{\partial \boldsymbol{u}_{\text{tot}}}, \boldsymbol{C}_{tot} = \frac{\partial \boldsymbol{g}}{\partial \boldsymbol{x}_{\text{tot}}}, \boldsymbol{D}_{tot} = \frac{\partial \boldsymbol{g}}{\partial \boldsymbol{u}_{\text{tot}}} \tag{5}$$

The matrices' numerical values $\boldsymbol{A_{tot0}}$, $\boldsymbol{B_{tot0}}$, $\boldsymbol{C_{tot0}}$, $\boldsymbol{D_{tot0}}$ are obtained by substituting the $\boldsymbol{x}_{\text{tot}}$ with the steady-state values $\boldsymbol{x}_{\text{tot}_0}$ obtained from the time-domain simulation.

2.6. *Modal analysis*

Modal analysis tools provide useful insights on how the different states interact with each, as well as the sensitivity of the modes to the system parameters. Such insights are very useful to understand the root cause of instabilities.

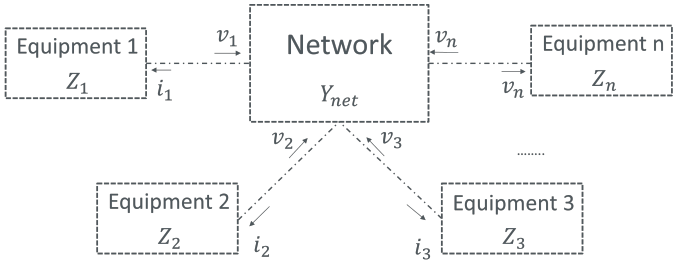

FIG. 3. Network equipment representation

2.6.1. *Eigenvalue analysis*

The state matrix, $\boldsymbol{A_{tot0}}$, provides information on the stability characteristics of the system. The stability of the system at the corresponding operating point is determined by computing the eigenvalues of the state matrix $\boldsymbol{A_{tot0}}$ [11]. The eigenvalues can be computed by solving the following equation

$$\det(\boldsymbol{A_{tot0}} - \lambda\mathbf{I}) = 0 \tag{6}$$

The characteristic equation is obtained by expanding the determinant in eq.6. The n roots of this characteristic equation represent the eigenvector $\boldsymbol{\lambda} = [\lambda_1, ..., \lambda_n]$. An eigenvalue λ is either a real number or a pair of conjugate complex values. When λ is a conjugate complex, it refers to an oscillatory mode, its imaginary part defines the oscillation frequency, and the real part governs the damping. In general, a mode λ is a global small-signal stability indicator, meaning that its is a property of the whole system including all apparatus and the network.

2.6.2. *State participation factor*

The right eigenvector $\boldsymbol{\phi}$ of size $n \times n$ is defined as

$$\boldsymbol{A_{tot0}}\boldsymbol{\phi} = dig(\boldsymbol{\lambda})\boldsymbol{\phi} \tag{7}$$

where $dig(\boldsymbol{\lambda})$ is the square diagonal matrix with the elements of vector $\boldsymbol{\lambda}$ on the main diagonal. Similarly, the left eigenvector $\boldsymbol{\psi}$ of size $n \times n$ satisfies

$$\boldsymbol{\psi}^T\boldsymbol{A_{tot0}} = \boldsymbol{\psi}^T dig(\boldsymbol{\lambda}) \tag{8}$$

The left and right eigenvectors are multiplied by each other producing a dimensionless matrix called the "participation matrix" $\boldsymbol{P}$, and the element $p_{ij} = \psi_{ij}\phi_{ij}$ is called participation factor which quantifies how much the i^{th} state variable contributes to the j^{th} mode, and vice versa. It is very useful to help identify which states are dominant in a particular oscillation.

2.6.3. *Other tools*

Other tools related to modal analysis, such as mode shape analysis, parameter sensitivity analysis are also included. Due to the limited scope of this paper, they are not discussed further.

2.7. *Impedance-based method*

Unlike modal analysis, which is a time-domain-based analysis method, the impedance-based method provides frequency-domain insight, making it intuitive to assess resonances and interaction modes. Besides, impedance models can be derived or measured for each equipment; therefore, a decentralized stability analysis can be conducted without requiring a global state-space model.

When applying the impedance-based method, the whole power network modelling is separated into two parts : network and equipment, as presented in Fig.3. The network is composed of DC cables, and its topology is defined by the spatial arrangement of the buses and the distances between them. Its dynamic behavior is represented by the nodal admittance matrix $\boldsymbol{Y_{net}}$, which can be derived from the branch data provided

in `MPC.branch`. The equipment includes all pieces of equipment, typically DC-DC converters, connected to the network's buses. The dynamic behavior of each piece of equipment is characterized by its corresponding output impedance, and together they form the output impedance matrix $\boldsymbol{Z_A}$, which is diagonal.

$$\boldsymbol{Z_A} = \begin{bmatrix} Z_1 & 0 & 0 \\ 0 & \ddots & 0 \\ 0 & 0 & Z_n \end{bmatrix} \tag{9}$$

From the small-signal point of view, the network and the equipment form a negative feedback system, as shown in Fig.4. The

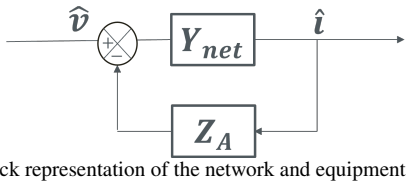

FIG. 4. Feedback representation of the network and equipment system

whole system's dynamic is represented by $\boldsymbol{Y_{sys}}$, referred to as the whole system admittance matrix, and defined as :

$$\boldsymbol{Y}_{\text{sys}} = \frac{\hat{\boldsymbol{i}}}{\hat{\boldsymbol{v}}} = (\boldsymbol{I} + \boldsymbol{Y}_{\text{net}}\boldsymbol{Z_A})^{-1}\boldsymbol{Y}_{\text{net}} \tag{10}$$

By using the Matlab function `feedback()`, $\boldsymbol{Y_{sys}}$ can be easily obtained. The elements of $\boldsymbol{Y_{sys}}$ are all transfer functions or impedance spectra, sharing a common set of poles which are identical to the eigenvalues obtained from modal analysis using the state-space model, as discussed in section 2.6.1. In fact, the diagonal element of $\boldsymbol{Y_{sys}}$ have a clear physical meaning. Taking the first diagonal element Y_{sys11} at bus-1 as an example, it is the inverse of the impedance of local equipment is series with the impedance of the grid seen from bus-1 [12, 13], i.e.,

$$\boldsymbol{Y_{sys11}} = (Z_{A1} + Z_{net1})^{-1} \tag{11}$$

This implies the possibility of using $\boldsymbol{Y_{sys}}$ for evaluating the system's stability at different locations corresponding to the global oscillatory mode.

3. TOOL VALIDATION

The developed tool is validated through three case studies. First, we provide a detailed discussion on its application to a simple 2-bus system, covering system construction, modal analysis, and the impedance-based method. Subsequently, we demonstrate how the tool can be applied to more complex multi-converter systems.

3.1. Case 1 : 2 bus system

To ensure the fundamental nature of the instability is not obscured by system complexity, we begin our analysis with a simple 2-bus system. This system comprises a DC-DC boost converter, a DC cable, and a DC-DC buck converter operating as a constant power load, as shown in Fig.5. The topology representation of such system is presented in Fig.6. Parameters related to the system and controller are summarized in Tab.5.

According to the whole system construction principle presented in subsection 2.3, the eletrical system in Fig.5 can be represented in Fig.7. Indeed, such a 2-bus system consists in total three individual elements : the DC cable, Boost DC-DC converter and buck DC-DC converter.

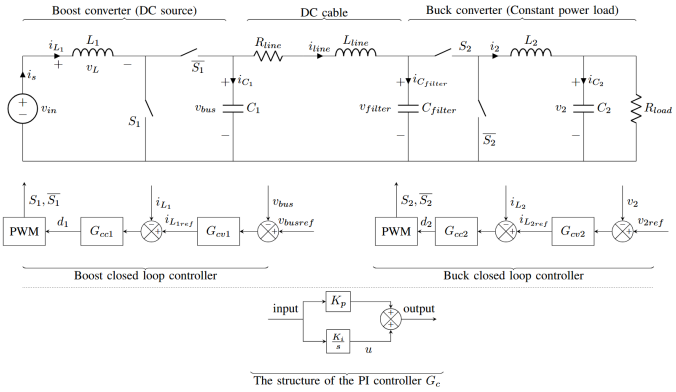

FIG. 5. Circuit diagram and controller of the 2-bus LVDC system

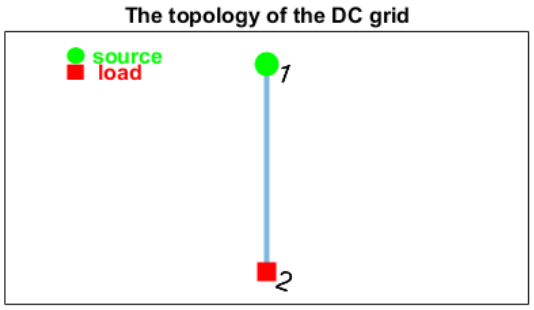

FIG. 6. Topology of the 2-bus LVDC system

3.1.1. DC cable

For the DC cable, its dynamic f_{line} is given as :

$$\begin{aligned} \frac{di_{line}}{dt} &= f_{line}(x_{line}, u_{g\_line}, \boldsymbol{p_{line}}) \\ &= \frac{(v_{bus} - v_{filter} - i_{line}R_{line})}{L_{line}} \end{aligned} \tag{12}$$

where, the global input is $u_{g\_line} = v_{bus} - v_{filter}$, the global output is $y_{g\_line} = i_{line}$, the state variable is $\boldsymbol{x_{line}} = [i_{line}] \in \mathbb{R}^1$, the line parameter $\boldsymbol{p_{line}} = [R_{line}, L_{line}]$.

3.1.2. DC-DC boost converter

For the boost converter, the closed-loop system's dynamics $\boldsymbol{f_{boost}}$ are described by the following :

$$\begin{aligned} \frac{di_1(t)}{dt} &= \frac{v_{in}(t) - (1-d_1)\, v_{bus}(t)}{L_1} \\ \frac{dv_{bus}(t)}{dt} &= \frac{(1-d_1)\, i_1(t) - i_{line}(t)}{C_1} \\ \frac{du_{cv1}(t)}{dt} &= K_{i_{cv1}}\left(v_{busref} - v_{bus}(t)\right) \\ \frac{du_{ci1}(t)}{dt} &= K_{i_{ci1}}\left(K_{p_{cv1}}\left(v_{busref} - v_{bus}(t)\right) + u_{cv1}(t) - i_1(t)\right) \end{aligned} \tag{13}$$

where the duty cycle d_1 is

$$d_1 = G_{ci1}\left(G_{cv1}\left(v_{busref} - v_{bus}(t)\right) - i_1(t)\right) \tag{14}$$

$G_{ci1} = K_{p_{ci1}} + \frac{K_{i_{ci1}}}{s}$ and $G_{cv1} = K_{p_{cv1}} + \frac{K_{i_{cv1}}}{s}$ are the PI current and voltage controllers, v_{busref} is the reference DC bus voltage. where $u_{cv1}(t)$ and $u_{ci1}(t)$ are output of the voltage controller's integral part and the output of the current controller's integral part, respectively. The global input is $u_{g\_boost} = -i_{line}$

TABLEAU 5. Circuit and controller parameters

Controller parameters	Circuit parameters
$K_{p_{ci1}}$=0.1235	v_{in}=24 V
$K_{i_{ci1}}$=210.78	R_{load}=6 Ω
$K_{p_{cv1}}$=0.3791	L_1=2200 μH
$K_{i_{cv1}}$=148.18	C_1=500μF
$K_{p_{ci2}}$=0.1221	R_{line}=0.087 Ω
$K_{i_{ci2}}$=221.644	L_{line}=3.318 μH
$K_{p_{cv2}}$=0.2159	C_{filter}=500 μF
$K_{i_{cv2}}$=49.8139	L_2=2200 μH
V_{2ref}, v_{busref}=24,48 V	C_2=2200 μF

and the global output is $y_{g\_boost} = v_{bus}$. The state variable vector is $\boldsymbol{x_{boost}} = [i_1, v_{bus}, u_{cv1}, u_{ci1}] \in \mathbb{R}^4$, the boost parameter $\boldsymbol{p_{boost}} = [v_{in}, L_1, C_1, K_{p_{ci1}}, K_{i_{ci1}}, K_{p_{cv1}}, K_{i_{cv1}}]$ and the local input is $u_{l\_boost} = v_{busref}$.

3.1.3. DC-DC buck converter

Buck converter's modeling is similar to that of the boost converter, and the closed-loop system's dynamics $\boldsymbol{f_{buck}}$ are

$$\begin{aligned} C_{filter}\frac{dv_{filter}}{dt} &= i_{line} - d_2 i_2(t) \\ L_2\frac{di_2(t)}{dt} &= d_2 v_{bus}(t) - v_2(t) \\ C_2\frac{dv_2(t)}{dt} &= i_2(t) - \frac{v_2(t)}{R_{load}} \\ \frac{du_{cv2}(t)}{dt} &= K_{i_{cv2}}\left(v_{2ref} - v_2(t)\right) \\ \frac{du_{ci2}(t)}{dt} &= K_{i_{ci2}}\left(K_{p_{cv2}}\left(v_{2ref} - v_2(t)\right) + u_{cv2}(t) - i_2(t)\right) \end{aligned} \tag{15}$$

where the duty cyle d_2 is given as

$$\begin{aligned} d_2 =& u_{ci2}(t) + K_{p_{ci2}}(K_{p_{cv2}}(v_{2ref} - v_2(t)) \\ &+ u_{cv2}(t) - i_2(t)) \end{aligned} \tag{16}$$

The voltage and current controllers are given as : $G_{cv2} = K_{p_{cv2}} + \frac{K_{i_{cv2}}}{s}$, $G_{ci2} = K_{p_{ci2}} + \frac{K_{i_{ci2}}}{s}$. $u_{cv2}(t)$ and $u_{ci2}(t)$ are the output of the voltage controller's integral part and the output of the current controller's integral part. The global input is $u_{g\_buck} = i_{line}$ and the global output is $y_{g\_buck} = v_{filter}$, $\boldsymbol{x_{buck}} = [v_{filter}(t), i_2(t), v_2(t), u_{cv2}(t), u_{ci2}(t)] \in \mathbb{R}^5$, the buck parameter $\boldsymbol{p_{buck}} = [C_{filter}, L_2, C_2, R_{load}, K_{p_{ci2}}, K_{i_{ci2}}, K_{p_{cv2}}, K_{i_{cv2}}]$ and the local input is $u_{l\_buck} = v_{2ref}$.

3.1.4. Construct the whole system

According to the topology of the 2-bus system, we can obtain that the global input of the DC cable is given by the difference between the global outputs of the boost and buck converters,i.e., $u_{g\_line} = v_{bus} - v_{filter} = y_{g\_boost} - y_{g\_buck}$. Simultaneously, the global input of the buck converter corresponds to the global output of the cable, i.e., $u_{g\_buck} = y_{g\_line}$, while the global input of the boost converter is the negative of the cable's global output, i.e., $u_{g\_boost} = -y_{g\_line}$. Fig.7 depicts the construction process of the whole system, which is completed automatically in the tool.

3.1.5. Modal analysis

Fig. 8 shows the location of the system's eigenvalues obtained from the modal analysis with the zoomed-in view of the low-frequency region. The dashed green and red lines represent

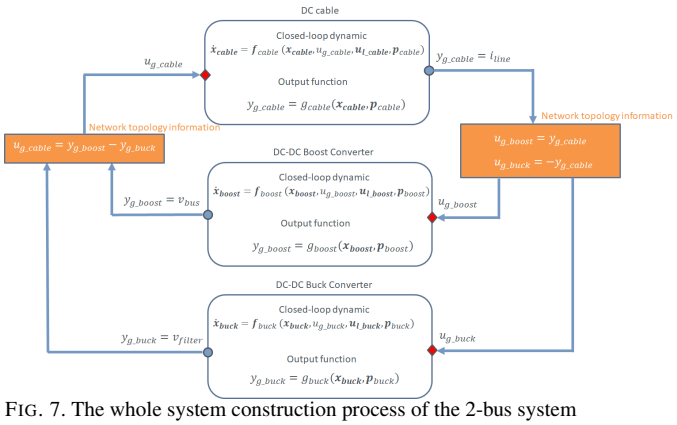

FIG. 7. The whole system construction process of the 2-bus system

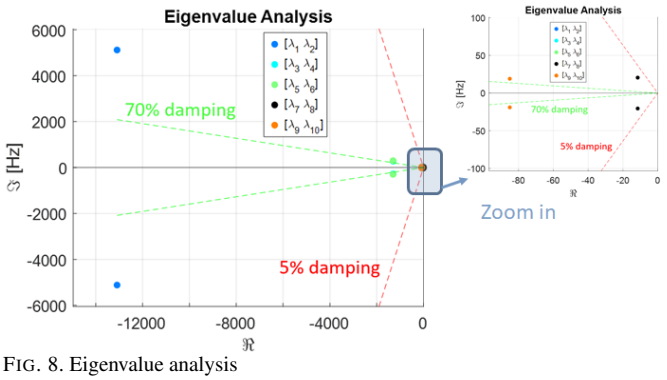

FIG. 8. Eigenvalue analysis

the boundaries where the eigenvalues have damping ratios of $\zeta = 0.7$ and $\zeta = 0.05$, respectively. It can be seen that the oscillatory mode ($\lambda_{7,8}$) associated with the boost voltage controller is located near the $\zeta = 0.05$ damping ratio boundary, indicating that this mode is poorly damped.

According to the participation factor analysis, the top three state variables contributing to this poorly oscillatory mode are $u_{cv1}, v_{bus}, v_{filter}$, indicating that this mode is associated with the voltage control loop of the boost converter, as shown in Fig.9. Therefore, it is possible to improve the stability by appropriately tunning the voltage loop parameters.

3.1.6. Impedance-based method

The bode diagram of Y_{sys11}, which is the first diagonal element of the whole-system admittance matrix is presented in Fig.10. Two resonant peaks appear in the bode plot, each representing an oscillation mode in the system. The peak at around 20Hz arises from the poorly damped oscillatory mode related to the voltage loop of the boost converter ($\lambda_{7,8}$ in Fig.8). The high-frequency peak, observed around 5000Hz, is attributed to the interaction between the converters' capacitances and the cable

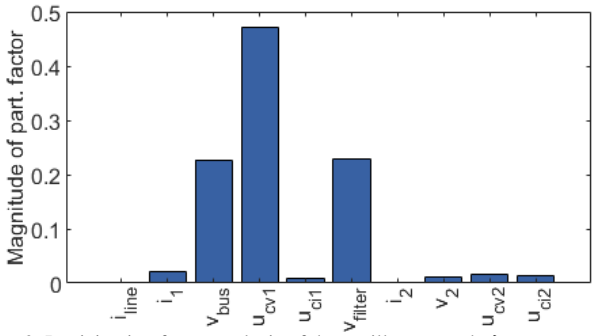

FIG. 9. Participation factor analysis of the oscillatory mode $\lambda_{7,8}$

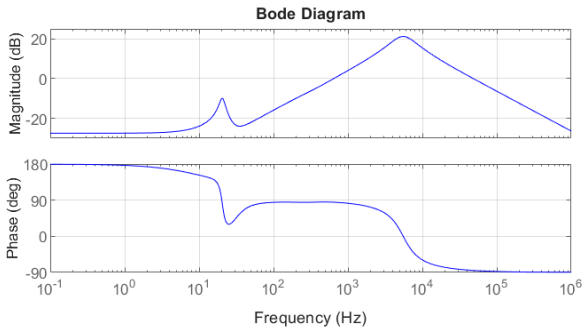

FIG. 10. Bode diagram of whole system admittance Y_{sys11} at bus-1

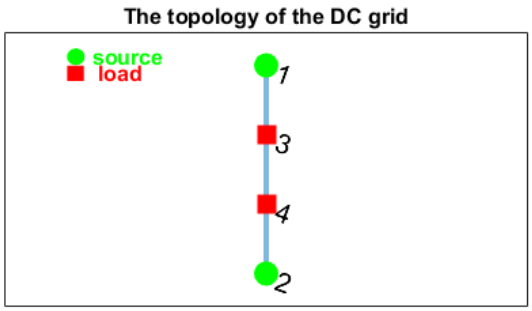

FIG. 11. Topology of the base system : a 4-bus symmetric LVDC system

inductance (C_1, L_{line}, C_2), this oscillatory mode corresponds to $\lambda_{1,2}$ in Fig.8.

3.2. *Case 2 : 4 bus system*

By extending the 2-bus system with two additional converters, a 4-bus system is formed, as shown in Fig.11. It consists of two identical areas connected through a cable. Each area includes one source converters (DC-DC boost converters with V-I droop control) and one constant power load (DC-DC buck converter), and the sources and load are interconnected by DC cable.

Fig.12 shows the location of system's eigenvalues obtained from the modal analysis toolbox. One can observe that the eigenvalues are distributed symmetrically, and all the eigenvalues are located at the left-half plane (LHP) of the complex plane, indicating that the system is stable.

3.3. *Case study 3 : 10 bus system*

The tool's applicability to analyze networks with complex topologies has also been tested, for example, a network with 10 bus and its eigenvalue analysis is shown in Fig.13

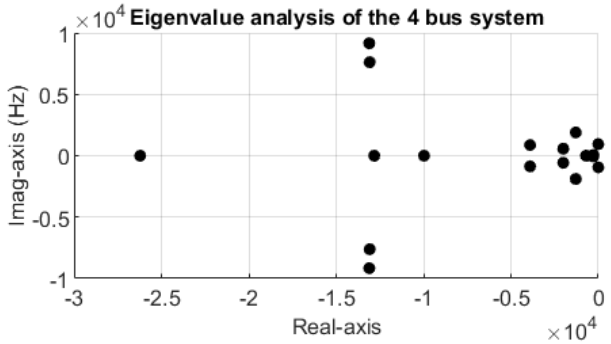

FIG. 12. The location of eigenvalues in nominal condition

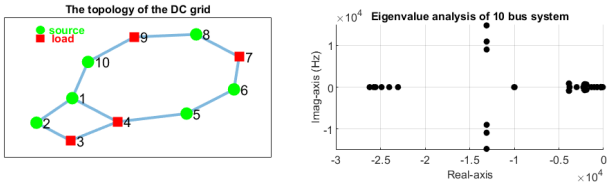

FIG. 13. DC network with 10 bus and its eigenvalue analysis

4. CONCLUSION

This paper presents a small-signal stability analysis tool specialized for Low Voltage DC (LVDC) network applications. The tool's design principle, including the individual components modelling and the whole system construction are presented in detail. The tool's effectiveness is validated by several case studies, ranging from simple to complex LVDC topologies. On the one hand, modal analysis provides a global aspect of the whole system's oscillatory modes in time-domain and helps identify states that contribute to specific oscillatory mode. On the other hand, the impedance-based method provides a local aspect of the frequency-domain information on specific buses. More functions, like eigenvalue decomposition and advanced parameter sensitivity, will be integrated.

5. REFERENCES

[1] R. D. Zimmerman, C. E. Murillo-Sánchez, and R. J. Thomas, "Matpower : Steady-state operations, planning, and analysis tools for power systems research and education," *IEEE Transactions on power systems*, vol. 26, no. 1, pp. 12–19, 2010.

[2] L. Thurner, A. Scheidler, F. Schäfer, J.-H. Menke, J. Dollichon, F. Meier, S. Meinecke, and M. Braun, "pandapower—an open-source python tool for convenient modeling, analysis, and optimization of electric power systems," *IEEE Transactions on Power Systems*, vol. 33, no. 6, pp. 6510–6521, 2018.

[3] F. Kelada, "An Open-Access Power System Linearization and EMT Simulation Tool." https://github.com/FKELADA/G2ELin, 2023.

[4] Y. G. Yitong Li, "Future-Power-Networks/Simplus-Grid-Tool." https://github.com/Future-Power-Networks/Simplus-Grid-Tool, 2024.

[5] F. Milano, "An open source power system analysis toolbox," *IEEE Transactions on Power systems*, vol. 20, no. 3, pp. 1199–1206, 2005.

[6] F. J. Cifuentes Garcia, T. Roose, C. Sakinci, D. Lee, L. Dewangan, E. Avdiaj, and J. Beerten, "Automated frequency-domain small-signal stability analysis of electrical energy hubs," in *2024 IEEE PES Innovative Smart Grid Technologies Europe (ISGT EUROPE)*, pp. 1–6, 2024.

[7] H. Cui, F. Li, and K. Tomsovic, "Hybrid symbolic-numeric framework for power system modeling and analysis," *IEEE Transactions on Power Systems*, vol. 36, no. 2, pp. 1373–1384, 2020.

[8] J. Sun, M. Xu, M. Cespedes, and M. Kauffman, "Data center power system stability—part i : Power supply impedance modeling," *CSEE Journal of Power and Energy Systems*, vol. 8, no. 2, pp. 403–419, 2022.

[9] S. Meunier, *Optimal design of photovoltaic water pumping systems for rural communities–a technical, economic and social approach*. PhD thesis, Université Paris Saclay (COmUE), 2019.

[10] L. Richard, *DC solar microgrids with decentralized production and storage for the Lateral Electrification of rural Africa*. PhD thesis, Université Grenoble Alpes, 2023.

[11] F. Kelada, J. Buire, and N. HadjSaid, "Revisiting small-signal modeling for analyzing fast dynamic interactions in converter-dominated power systems," *IEEE Transactions on Power Systems*, 2025.

[12] Y. Zhu, T. C. Green, X. Zhou, Y. Li, D. Kong, and Y. Gu, "Impedance margin ratio : a new metric for small-signal system strength," *IEEE Transactions on Power Systems*, 2024.

[13] Y. Zhu, Y. Gu, Y. Li, and T. C. Green, "Participation analysis in impedance models : The grey-box approach for power system stability," *IEEE Transactions on Power Systems*, vol. 37, no. 1, pp. 343–353, 2021.